

# Efficiency Study of the Non-Instantaneous Double Support Phase in HZD Controlled Bipedal Robot

Yinnan Luo<sup>1</sup>, Ulrich J. Römer<sup>1</sup>, Marten Zirkel<sup>2</sup>, Lena Zentner<sup>2</sup>, and Alexander Fidlin<sup>1</sup>

<sup>1</sup> Institute of Engineering Mechanics, Karlsruhe Institute of Technology, Karlsruhe, Germany

<sup>2</sup> Compliant Systems Group, Ilmenau University of Technology, Ilmenau, Germany

**Abstract.** A study on the influence of a non-instantaneous double support phase on the energy efficiency and the stability of a bipedal walking robot with hybrid zero dynamics control is performed. The planar robot model consists of five rigid body segments and four actuated revolute joints. The periodic gait includes two alternating continuous single and double support phases as well as two discrete transition events. Two virtual actuators are introduced to create one degree of under-actuation in the double support phase. Periodic solutions of the gait are found via the numerical optimization, which minimizes the energy consumption of locomotion. The resulted efficiency and stability are compared against the common model approach with instantaneous double support phase. Despite the less efficiency, the extended controller with non-instantaneous double support phase improves the gait stability, which could be beneficial for the experimental validation on a robot prototype.

**Keywords:** Bipedal Walking Robot, Double Support Phase, Hybrid Zero Dynamics Control.

## 1 Introduction

The development of humanoid robots has been rapidly progressed in recent years. For humanoids, bipedal walking is one of the most important movement patterns for the locomotion in varying environments. In order to simplify the task of creating stable gaits, different model approaches have been suggested [1]. Bipedal gaits are usually divided into two alternating phases: a single support phase (SSP) and a double support phase (DSP). In the SSP, the robot touches the ground only with a single stance leg; and the other leg swings forward without interaction with the environment. In the DSP, both feet contact the ground.

In order to design a controller, different assumptions regarding the DSP duration were suggested. A widespread control strategy is based on the zero moment point (ZMP) concept [2], which is mostly applied in robotic systems that contain a large number of actuated degrees of freedom (DoF). Due to the high flexibility, the DSP is easily handled as a continuous dynamical process in

the similar sense like the SSP [3, 4]. In contrast, control strategies based on the hybrid zero dynamics (HZD) approach are developed for under-actuated robots, whose motion is generated by fewer actuators [5, 6]. The controller synchronizes the actuated DoF to a set of the parameterized reference trajectories. Thus the remaining under-actuation yields the internal dynamics of the controlled system. Periodic gaits can be analyzed by studying the limit cycle of the zero dynamics—the internal dynamics when there is no deviation from the reference trajectories. The vast majority of HZD controller in the literature assume an instantaneous DSP where the former swing leg impacts the ground and the former stance lifts off. This gives a hybrid model for walking as a periodic sequence of continuous SSPs and discrete phase transitions that include the DSP [7–9]. So far there has been little researches [10] into extending the HZD control approach to consider a DSP with finite duration. Since there are more constraints in the DSP than in the SSP, fewer actuators are required in the DSP. In the present manuscript, we study the influence of a non-instantaneous DSP on the efficiency and stability of the walking gaits.

The paper has the following structure: Section 2 briefly introduces the robot model and the related HZD control; Section 3 discusses the optimization results of the efficiency study and compares different model approaches; Section 4 concludes the study with a summary and outlook.

## 2 Robot Model and Control Design

The investigated planar robot model in Fig. 1 consists of five rigid body segments, which are connected over four revolute joints. Electric drive trains are integrated into each joint to provide the driving torque for control. Point feet are assumed at the end of the legs, thus the non-slipping stance foot is modelled as a frictionless pivot. At a constant walking speed (step length over step duration  $\ell_{\text{step}}/t_{\text{step}}$ ), the gait consisting of alternating single and double support phases is periodic. Both SSP and DSP are continuous and described by ordinary differential equations. The transition between them is accomplished via discontinuous events, namely an inelastic impact when the swing leg touches the ground, and the lift-off of the trailing leg. Therefore, the periodic walking gait is represented by the alternating sequence composed of DSP  $\rightarrow$  lift-off  $\rightarrow$  SSP  $\rightarrow$  touch down.

During the DSP (Fig. 1 left), both feet are constrained on the ground, thus the step length  $\ell_{\text{step}}$  remains constant. In this configuration, two legs form a closed kinematic chain and the model has 3 DoF. The independent coordinates<sup>3</sup> are  $\mathbf{q}_d := [\theta, \mathbf{q}_{di}^\top]^\top$  with  $\mathbf{q}_{di} := [\theta_{H1}, \theta_{K1}]^\top$ , therefore the trailing leg  $\mathbf{q}_{dd} := [\theta_{H2}, \theta_{K2}]^\top$  can be expressed as a function  $\mathbf{q}_{dd}(\mathbf{q}_d)$  using the geometric relations of the closed kinematic chain. Since four actuators  $\mathbf{u} := [u_{H1}, u_{H2}, u_{K1}, u_{K2}]^\top$

---

<sup>3</sup>Here, the straight line connecting the hip joint and the front stance foot represents the virtual leg to define the absolute body orientation  $\theta$  in the DSP, as depicted in Fig. 1 left. In the SSP, however, the virtual leg is defined by the straight line that connects the hip joint and the stance foot.

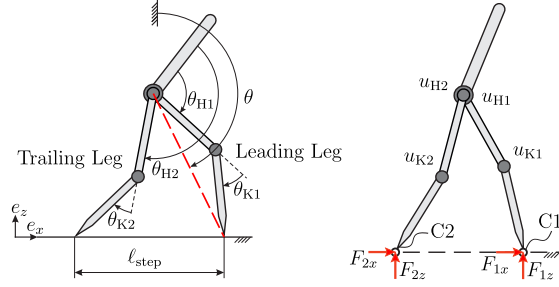


**Fig. 1.** Left: five link robot model and coordinates in the DSP. Right: four electric motors in the joint and the reaction forces on feet in the DSP.

are available, the DSP is over-actuated. The equation of motion is

$$\mathbf{M}_d \ddot{\mathbf{q}}_d + \boldsymbol{\Gamma}_d = \mathbf{B}_d \mathbf{u} , \quad (1)$$

with the inertia matrix  $\mathbf{M}_d$ , the generalized force  $\boldsymbol{\Gamma}_d$  including the gravitational and Coriolis force and the input matrix  $\mathbf{B}_d$  derived by means of virtual works. In order to create an under-actuated DSP, two independent virtual actuators  $\tilde{\mathbf{u}} := [\tilde{u}_1, \tilde{u}_2]^\top$  are projected onto the physical actuators  $\mathbf{u}$  through the projection matrix  $\mathbf{P}_d$ <sup>4</sup> of the dimension  $(4 \times 2)$  by  $\mathbf{u} = \mathbf{P}_d \tilde{\mathbf{u}}$ . Consequently, the HZD control from [5] can be applied for the DSP, which is combined with the SSP to model the entire gait, as in this case both DSP and SSP have one DoF under-actuation.

The detailed control design is addressed in [11], which develops three different control concepts in order to deal with the over-actuated DSP. This manuscript uses the controller that artificially creates an under-actuated DSP via projection  $\mathbf{P}_d$ . The controller in the DSP synchronizes the actuated joints to a set of reference trajectories  $\mathbf{q}_{d,\text{ref}}(\theta, \boldsymbol{\alpha}_d)$ , that are parametric functions (Bézier curves) with parameters  $\boldsymbol{\alpha}_d$ . These are equidistant control points that determine the shape of the Bézier curve and thus parameterize the reference trajectory. Instead of time, the phase angle  $\theta$  is regarded as the independent variable, since  $\theta$  monotonously increases during both SSP and DSP. The method of input-output linearization combined with a PD controller ( $\mathbf{v} = -\mathbf{K}_P \mathbf{y} - \mathbf{K}_D \dot{\mathbf{y}}$ ) zeroes the control output  $\mathbf{y} = \mathbf{q}_{di} - \mathbf{q}_{d,\text{ref}}(\theta, \boldsymbol{\alpha}_d)$ . Positive definite gains  $\mathbf{K}_P$  and  $\mathbf{K}_D$  ensure the asymptotic stability of  $\mathbf{y}$ . The controller in the SSP has the same design, but is applied for four actuated joints.

As the study focuses on the efficiency of locomotion, the reference motion without control error ( $\mathbf{y} \equiv \mathbf{0}$ ) is simulated. The dynamics of the controlled system are reduced to the remaining zero dynamics  $\dot{\mathbf{z}} = \mathbf{f}_{\text{zero}}(\mathbf{z})$  with  $\mathbf{z} := [\theta, \sigma]$ , where  $\sigma$  is the generalized momentum conjugate to  $\theta$ . The periodic gaits, including the discrete transition events, can thus be described by the limit cycle

<sup>4</sup>The projection  $\mathbf{P}_d = [\mathbf{P}_{d,1}, \mathbf{P}_{d,2}]$  is regarded as gaits parameters with the restrictions  $|\mathbf{P}_{d,1}| - 1 = 0$ ,  $|\mathbf{P}_{d,2}| - 1 = 0$ , and  $\mathbf{P}_{d,1} \cdot \mathbf{P}_{d,2} = 0$ , which are formulated as equality constraints in the numerical optimization in the efficiency study.

of the dynamics of the hybrid system, whose solution is determined via numerical optimization. Its objective is to minimize the energy consumption, which is evaluated by the cost of transport ( $CoT := E_{\text{supp}}/(\ell_{\text{step}} \cdot mg)$ ) with the total supplied energy  $E_{\text{supp}}$ , the step length  $\ell_{\text{step}}$  and the robot weight  $mg$ . A Sequential Quadratic Programming (SQP) algorithm from *Artelys Knitro* is used to solve the constrained optimization.

### 3 Efficiency and Stability Study

The major goal of the present research is to gain insight into the influence of the continuous DSP on the efficiency of bipedal walking. For this purpose, section 3.1 addresses the efficiency of different configurations for formulating an under-actuated DSP; subsequently in section 3.2, walking with non-instantaneous DSP is compared to a common HZD controller with instantaneous DSP.

#### 3.1 Comparison of Controllers with Non-Instantaneous DSP

The efficiency is studied for each individual walking speed in the range  $\mathbf{v} := [0.2, \dots, 1.4]^T$  m/s. According to section 2, different under-actuated DSPs can be achieved by varying  $\mathbf{P}_d$ , whose optimum  $\mathbf{P}_d = \mathbf{P}_{d,\text{opt}}$  is plotted in Fig. 2 (top)<sup>5</sup>. Here the (4, 2)th entry of the matrix  $\mathbf{P}_{d,\text{opt}}$  (denoted as  $\mathbf{P}_{d,\text{opt}}^{(4,2)} \approx 1$ ) remains nearly constant<sup>6</sup>, meaning a dominating projection of the virtual input  $\tilde{u}_2$  onto the trailing leg’s knee during the DSP for all speeds. The optimum selection of the hip actuators depends on the velocity: the leading leg hip motor  $u_{H1}$  should be actuated for faster walking ( $v \geq 0.8$  m/s); otherwise, the trailing leg hip motor  $u_{H2}$ . The reason behind is that the optimum efficient gait differs while the velocity changes. For instance, the hip joints experience larger displacements at 1.4 m/s in comparison to 0.4 m/s, as illustrated in Fig. 2 (bottom).

Two other configurations  $\mathbf{P}_{d,\text{Front}}$  and  $\mathbf{P}_{d,\text{Back}}$  with

$$\mathbf{P}_{d,\text{Front}} = \begin{bmatrix} 1 & 0 \\ 0 & 0 \\ 0 & 1 \\ 0 & 0 \end{bmatrix} \quad \text{and} \quad \mathbf{P}_{d,\text{Back}} = \begin{bmatrix} 0 & 0 \\ 1 & 0 \\ 0 & 0 \\ 0 & 1 \end{bmatrix}$$

are considered in the efficiency study. The aim is to analyze the effect of the actuation that is provided from different joints in an under-actuated DSP. Indeed,  $\mathbf{P}_{d,\text{Front}}$  and  $\mathbf{P}_{d,\text{Back}}$  involve no virtual actuators in the sense of the control design described in section 2. Instead, they simply activate two physical actuators that are located either in the front ( $\mathbf{P}_{d,\text{Front}}$ ) or the back leg ( $\mathbf{P}_{d,\text{Back}}$ ),

<sup>5</sup>Note that this projection is not related in the SSP, since the system has five DoF and all four actuators are required for creating the under-actuation of one DoF.

<sup>6</sup>This implicitly means that  $\mathbf{P}_{d,\text{opt}}^{(i,2)} \approx 0$  for  $i \in [1, 2, 3]$ , due to the requirement  $|\mathbf{P}_{d,2}| - 1 = 0$  from section 2. After the DSP is terminated, however, all actuators provide driving torques for the walking motion in the following SSP.

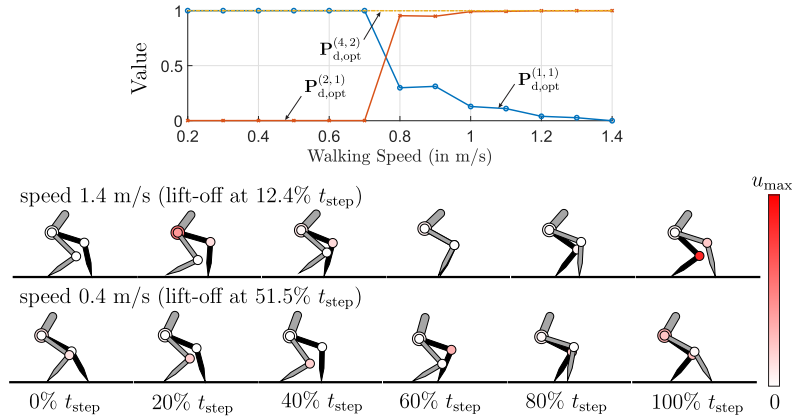


**Fig. 2.** Top: Optimized elements in the projection matrix  $\mathbf{P}_{d,opt}$ . Bottom: Walking gaits of a step, containing the sequence of DSP  $\rightarrow$  lift-off  $\rightarrow$  SSP  $\rightarrow$  touch down, produced by the optimal projection  $\mathbf{P}_{d,opt}$  during the DSP. The front leg in the DSP and the stance leg in the SSP are colored black.

which is the most straightforward way to create one degree of under-actuation in the DSP. Despite the conceptual difference, the optimum energy consumption of all three motor selections are compared in Fig. 3. Differences between the optimum projection  $\mathbf{P}_{d,opt}$  and  $\mathbf{P}_{d,Back}$  can be observed at  $v < 0.8$  m/s, where the hip motor  $u_{H2}$  in the trailing leg mainly decelerates the motion and thus produces more heat losses. Since periodic gaits can be regarded as limit cycles of the controlled system, the total energy level remains constant. All energy losses—including the heat loss in the generator mode of the actuator and the inelastic impact loss of the swing leg—must be supplied during the continuous phases. The impact loss is minimized implicitly by the optimization. Specifically, electric motors are involved to slow down the optimum motion right before the collision in order to reduce this loss. However, the deceleration process produces heat losses, which significantly affect the efficiency. At 0.4 m/s, 27% of the total heat losses are generated in the DSP due to  $\mathbf{P}_{d,Back}$ ; On the other hand, the heat loss proportion in the DSP is reduced to 12% by selecting  $\mathbf{P}_{d,opt}$ . Thus, the unnecessary deceleration is avoided by the optimum motor selections which improves the efficiency.

Activating the leading leg through  $\mathbf{P}_{d,Front}$  produces the worst efficiency. Its drawback is that the relative DSP duration cannot be adjusted to match the optimum for a large range of speeds, as plotted in Fig. 4 (left). Since the step length  $\ell_{step}$  from optimizing all scenarios in Fig. 3 is of similar magnitude ( $\ell_{step,min} = 0.35$  m,  $\ell_{step,max} = 0.46$  m), the DSP could be utilized to delay the step in order to reach a lower target speed. In fact, with the optimum gait in Fig. 2 (bottom), 52% of the step period at 0.4 m/s takes place in the DSP, and only 12% at 1.4 m/s. This could be an advantage in application scenarios, where the velocity must be varied in a large range but the step length is constrained

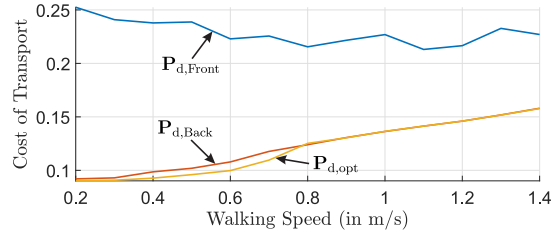


**Fig. 3.** Optimized cost of transport ( $CoT$ ), resulted from different control assumptions, over the speed range  $\mathbf{v} := [0.2, \dots, 1.4]^T$  m/s.

through environmental conditions, for example when climbing stairs with constant geometry. Another aspect to explain the efficiency difference is to analyze the mechanical work input of the actuators during the DSP. In other words, the sub-optimum motor selection would solely create heat losses in its generator mode, e.g.  $\mathbf{P}_{d,Front}$  in Fig. 4 (right). However, despite the negligible contribution from the front leg actuators, they are necessary to fulfill the constraints in the DSP.

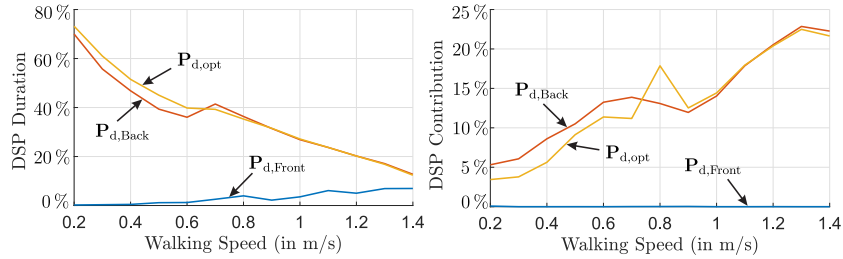


**Fig. 4.** Left: The relative duration of the DSP in the entire step period. Right: Energy consumption that is caused during the DSP in relation to the total step.

Creating an under-actuated DSP by only using two hip or two knee actuators makes it difficult for the optimization to find feasible solutions. In the first case, the inequality constraints on the stance foot (such as non-slipping) can be barely fulfilled by the hip actuation over the knees that are rotating freely. On the other hand, by actuating only the knee joints, it is no longer possible to control the upper body, since both hip joints are unactuated. Thus, these scenarios are excluded from the present efficiency study.

### 3.2 Comparison of Non-Instantaneous and Instantaneous DSP

The optimized efficiency of ( $\mathbf{P}_d = \mathbf{P}_{d,opt}$ ) from section 3.1 is compared against the results of a common HZD controller with a continuous SSP and an instantana-

neous DSP. According to the result in Fig. 5, gaits with the instantaneous DSP achieve the highest efficiency: The average  $CoT$  is 68% less than the optimum with a non-instantaneous DSP. In order to explain the large gap between these two efficiency results, two additional restrictions are considered when creating the instantaneous DSP gait.

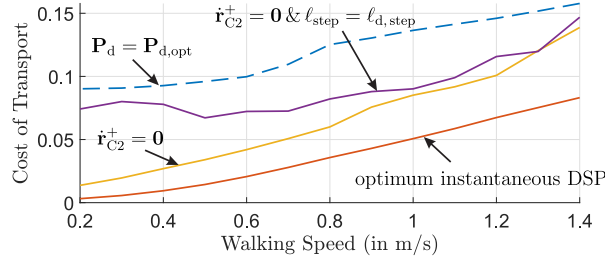


**Fig. 5.** Optimized cost of transport of different model assumptions, including gaits containing a non-instantaneous DSP (dashed line) or an instantaneous DSP (solid lines).

According to the hypothesis in [5], the swing leg lifts off immediately after the impulsive collision with the non-zero velocity. This differs from the model with non-instantaneous DSP, where the lift-off velocity of the swing foot is zero at the beginning of the SSP. Thus, the first modification requires the swing foot velocity to be  $\dot{\mathbf{r}}_{C2}^+ = \mathbf{0}$  at the beginning of the SSP. Moreover, it was observed from previous studies in [7, 12] that the optimum step length of the instantaneous DSP gait almost linearly correlates with the walking speed. This correlation is not observed from non-instantaneous DSP gaits, as discussed above. Therefore, the second modification sets the step length of the optimum non-instantaneous DSP gait equal to that of the instantaneous DSP at every speed. As shown in Fig. 5, these additional restrictions indeed require more energy consumption and reduce the efficiency gap. However, differing from the walking pattern in Fig. 6, the robot in Fig. 2 (bottom) tends to tilt its upper body towards the walking direction to create the forward motion, which needs larger decelerating operations from the motor to hold the upper body after each collision with much worse efficiency. Also noticeable from Fig. 2 (bottom) is the heavily bowed knee joints, which are necessary for the robot to control the contact force in order to avoid slipping during the non-instantaneous DSP. This requires much more power provided from the actuator, instead of utilizing free oscillations of the body segment depicted in Fig. 6.

The other aspect of the comparison is the stability of the periodic gaits affected by the controller. First of all, the asymptotic stability of the control error between the actuated joint angle and its reference is provided by the high gain PD controller, which is furthermore necessary for rendering the asymptotic stability of the periodic solution of the hybrid zero dynamics, in other

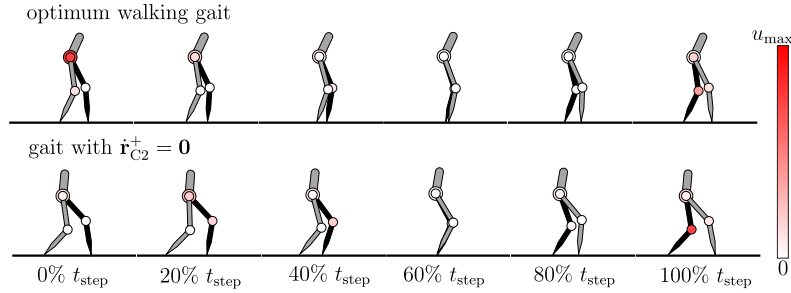


**Fig. 6.** Walking gaits starting with the SSP and ending with the inelastic impact at 1.4 m/s. The stance leg is colored black.

words, the under-actuated DoF of the controlled system. This is evaluated by the Floquet-multiplier  $\Lambda$ , which is derived from the Poincaré map of the hybrid zero dynamics’ periodic solution<sup>7</sup>. The non-instantaneous DSP significantly improves the stability property of the HZD’s limit cycle for most of the investigated speeds  $v < 1.4$  m/s, since it generates much smaller Floquet multipliers, cf. Fig. 7. Consequently, solutions with any small initial deviations or external perturbations have a much faster convergence rate towards the reference limit cycle—the steady walking gait of the robot at a constant speed.

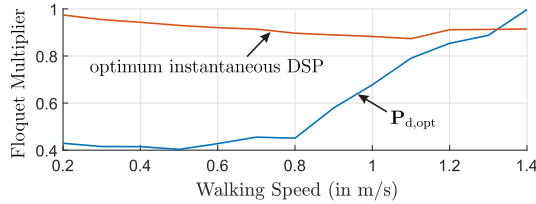


**Fig. 7.** Floquet multipliers derived from different DSP approaches.

In order to transfer the simulated gaits to a real robot prototype, one of the most challenging tasks is to set up proper initial conditions for the experiment, including angle and angular velocity of all body segments, before reaching a steady periodic gait. Thus a closed loop simulation of the robot with the PD feedback is occupied for the two different DSP assumptions<sup>8</sup>. The initial condition of all angles is assumed equal to that of the reference limit cycle, but the initial angular velocities in all body joints are set to zero. Fig. 8 depicts

<sup>7</sup>The method for determining the solution as well as calculating the Floquet-multiplier is developed in [9, 11]. The solution is stable if  $0 < \Lambda < 1$ .

<sup>8</sup>This comparison considers the simplest control law with the linear PD feedback to study the stability. Introducing nonlinear feedback laws could enhance the convergence towards the limit cycle. This is, however, not the focus of the presented work.



the evolution of the corresponding internal dynamics displayed by the coordinates  $[\theta, \sigma]$ . Due to the PD feedback, the instantaneous DSP gait (Fig. 8 left) slowly approaches the limit cycle requiring a lot of steps. In contrast, the non-instantaneous DSP (Fig. 8 right) shows much faster convergence, which would simplify the process of initializing the experimental operation<sup>9</sup>.

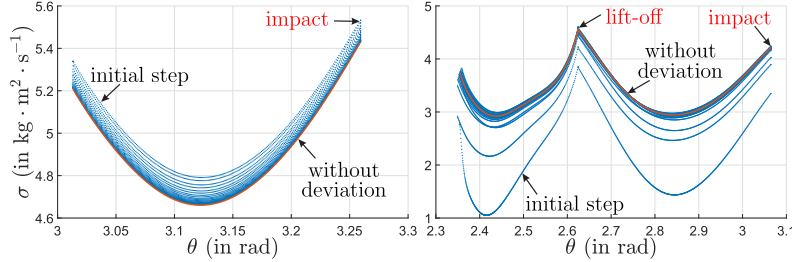


**Fig. 8.** Closed loop simulation with zero initial joint velocities for instantaneous DSP (left) and non-instantaneous DSP (right) at 0.6 m/s.

## 4 Conclusion

In the presented study, the control design and its effect on the efficiency of walking of a planar five segment bipedal robot is investigated. The hybrid zero dynamics control is extended for periodic gaits that consist of alternating continuous single and double support phases. Transitions between the continuous phases occur in the form of two discontinuous events: the lift-off of the trailing leg and the touch down of the swing leg. In the non-instantaneous double support phase, both feet stay on the ground without slipping. Therefore, the model has more actuators than degrees of freedom, meaning it is over-actuated. In order to reduce the number of independent actuators, two virtual inputs are introduced and projected onto the four physical actuators. Consequently, the hybrid zero dynamics control which utilizes one degree of freedom of under-actuation is applied in both phases. A numerical optimization process is used to find the periodic solution of the gait and to optimize the virtual actuator projection and the other gait parameters, with the aim of minimizing the energy consumption of locomotion.

According to the optimization results for a range of different walking speeds, the trailing leg knee should always be actuated during the double support phase. Whether the second active actuator should be in the leading or trailing leg's hip joint depends on the walking speed. Furthermore, the optimum gaits are

<sup>9</sup>Also, using all actuators in the over-actuated DSP provides many possibilities to formulate other control tasks, such as the direct control on the generalized momentum for even better stability [11].

compared to the results with an instantaneous double support phase. Despite being less efficient, the controller with non-instantaneous double support phase offers opportunities to enhance the gait stability, which might be beneficial for experiments on a robot prototype. One of the essential reasons of the poor efficiency of the gait with the non-instantaneous double support phase is that the point foot is modelled at the end of the lower leg. As a counterexample, humans are able to utilize their foot rolling on the ground to produce high efficient gaits during the non-instantaneous DSP.

**Acknowledgements:** This work is financially supported by the German Research Foundation (DFG), grant FI 1761/4-1 | ZE 714/16-1.

## References

1. J. Reher, and A.D. Ames. “Dynamic Walking: Toward Agile and Efficient Bipedal Robots”. *Annual Review of Control, Robotics, and Autonomous Systems*. 4. pp. 535-572 (2021).
2. H. Tran Thien, C. Van Kien, and H.P.H. Anh. “Optimized stable gait planning of biped robot using multi-objective evolutionary JAYA algorithm”. *International Journal of Advanced Robotic Systems*. 17(6). (2020).
3. R. Rajendra, and D. Pratihari. “Analysis of double support phase of biped robot and multi-objective optimization using genetic algorithm and particle swarm optimization algorithm”. *Sadhana*. 40. pp. 549–575 (2015).
4. T. Li et al., “Stability control for biped walking based on phase modification during double support period”, *2014 IEEE International Conference on Robotics and Biomimetics (ROBIO 2014)*, pp. 1290-1295 (2014).
5. E.R. Westervelt, J.W. Grizzle, and D. Koditschek, “Hybrid Zero Dynamics of Planar Biped Walkers”, *IEEE Transactions on Automatic Control* 48(1), pp. 42–56 (2003).
6. E.R. Westervelt, J.W. Grizzle, C. Chevallereau, J.H. Choi, and B. Morris, *Feedback Control of Dynamic Bipedal Robot Locomotion*. Boca Raton: CRC press. (2007).
7. F. Bauer, U.J. Römer, A. Fidlin, and W. Seemann, “Optimization of energy efficiency of walking bipedal robots by use of elastic couplings in the form of mechanical springs”, *Nonlinear Dynamics* 83(3), pp. 1275–1301 (2015).
8. F. Bauer, U.J. Römer, A. Fidlin, and W. Seemann, “Optimal elastic coupling in form of one mechanical spring to improve energy efficiency of walking bipedal robots”, *Multibody System Dynamics* 38(3), pp. 227–262 (2016).
9. U.J. Römer, C. Kuhs, M.J. Krause, and A. Fidlin, “Simultaneous optimization of gait and design parameters for bipedal robots”, *2016 IEEE International Conference on Robotics and Automation (ICRA)* pp. 1374-1381 (2016).
10. K.A. Hamed, N. Sadati, W.A. Gruver, and G.A. Dumont, “Stabilization of Periodic Orbits for Planar Walking With Noninstantaneous Double-Support Phase”. *IEEE Transactions on Systems, Man, and Cybernetics - Part A: Systems and Humans*, 42, pp. 685-706 (2012).
11. Y. Luo, U.J. Römer, A. Dyck, M. Zirkel, L. Zentner and A. Fidlin, “Hybrid Zero Dynamics Control for Bipedal Walking with a Non-Instantaneous Double Support Phase”. *arXiv*, (2023, Preprint available: <https://arxiv.org/abs/2303.05165>).
12. Y. Luo, U.J. Römer, L. Zentner and A. Fidlin, “Improving Energy Efficiency of a Bipedal Walker with Optimized Nonlinear Elastic Coupling”. *Advances in Nonlinear Dynamics. NODYCON Conference Proceedings Series*. pp. 253–262 (2022).